Z. Phys. Chem. **219** (2005) 877–890
© by Oldenbourg Wissenschaftsverlag, München

Dry-Gel Synthesis of Mesoporous MCM-41 Materials with Modified Pore Structure

By Mingcan Xu, Wei Wang, Jens Weitkamp, and Michael Hunger*

Institute of Chemical Technology, University of Stuttgart, D-70550 Stuttgart, Germany

Dedicated to Prof. Dr. Helmut Knözinger on the occasion of his 70th birthday

(Received February 18, 2005; accepted March 1, 2005)

Dry-Gel Conversion Method / Mesoporous MCM-41 Material / Zeolite ZSM-5 / Brønsted Acidity / Solid State NMR Spectroscopy

For the first time, the dry-gel conversion method was applied for the preparation of MCM-41 materials with partially crystalline framework. The X-ray diffraction pattern of the material obtained after a dry-gel conversion time of 36 h consists of reflections of both long-range ordered MCM-41 material and zeolite ZSM-5. The nitrogen adsorption/desorption isotherm confirms the presence of micropores and uniform mesopores with a narrow pore size distribution. By ^{29}Si MAS NMR spectroscopy it was evidenced that a significant portion of the amorphous MCM-41 framework was transformed into a partially crystalline framework. TEM and SEM images indicate the occurrence of mesopores with disturbed arrangements, but no formation of separate zeolite ZSM-5 crystals occurred. By ^{1}H MAS NMR spectroscopy of the above-mentioned material, the formation of hydroxyl groups with a chemical shift of *ca.* 4 ppm and a concentration of *ca.* 0.1 mmol/g was observed. The acid strength of these hydroxyl groups, as studied by adsorption of the ^{13}C MAS NMR probe molecule ^{13}C-2-acetone, was found to agree with that of bridging OH groups in zeolite H-ZSM-5. After conversion times of 48 h and 72 h, an extensive to total transformation of the dry gel into zeolite ZSM-5 occurred.

1. Introduction

Due to the uniform mesopores and the large specific surface area of mesoporous MCM-41 materials [1, 2], these porous solids have attracted wide attention for applications in adsorption and heterogeneous catalysis [3–5]. Its amorphous framework, the poor hydrothermal stability and the weak Brønsted acidity, however, are strong limitations for industrial applications.

* Corresponding author. E-mail: michael.hunger@itc.uni-stuttgart.de

Consequently, much effort has been devoted to overcoming these disadvantages [6–13]. Recently, progress has been made in enhancing both the hydrothermal stability and the acid strength of MCM-41 materials. Mesoporous MCM-41 materials modified with $AlCl_3$ showed a much higher acid strength than the as-synthesized [Al]MCM-41 [8–10]. Hydrothermally stable mesoporous MCM-41 materials were synthesized by Zhang *et al.* [11] and Liu *et al.* [12, 13] by a combination of a zeolite seed synthesis with a preparation of mesoporous materials using micelles as templates.

According to Liu *et al.* [13], the hydrothermal stability of MCM-41 materials can be strongly improved by a hydrothermal synthesis using cetyltrimethylammonium bromide (CTAB) to template a 'zeolite seed' solution, which was prepared by tetrapropylammonium hydroxide (TPAOH) as template. The improved hydrothermal stability was explained by a formation of zeolite subunits in the framework of the obtained [Al]MCM-41 material. This material retained well-ordered mesopores after a high-temperature hydrothermal treatment, even upon steaming at a temperature of 1073 K [13]. Despite the reported higher activity of this material for cumene conversion in comparison with conventionally synthesized MCM-41, no zeolite-like acid sites were observed [13].

The transformation of the amorphous [Al]MCM-41 framework into a material with a partially crystalline structure could be an approach to introduce Brønsted acid sites, while maintaining the mesopores [14]. However, strongly basic conditions are required for the crystallization of zeolites [15], which would damage the MCM-41 framework under the conditions of a conventional hydrothermal zeolite synthesis. This incompatibility frustrated many attempts to obtain mesoporous materials with a partially crystalline framework. In recent works, mixtures of mesoporous materials and zeolites or MCM-41/ZSM-5 composites consisting of so-called connected microporous and mesoporous materials were obtained [14, 16]. These materials were synthesized by using a mixed template method or a two-step crystallization process.

The dry-gel conversion is a useful tool for the synthesis of zeolites with uniform particle size and for the incorporation of metals into the zeolite framework [17–19]. As observed by Matsukata *et al.* [18], the shapes of the parent dry gel particles are mostly retained upon the crystallization of zeolites. This is explained by the hindered dissolution processes in the dry gel due to the limited water content.

In the present work, mesoporous materials with modified pore structure were prepared using a gel suitable for the synthesis of zeolite ZSM-5 seeds. After an aging of this gel, it was added to a solution of cetyltrimethylammonium bromide to reach an ordered hexagonal arrangement of the inorganic compounds. Subsequently, the gel was dried leading to a powdered dry gel. Via the dry-gel conversion process, mesoporous materials with different contents of zeolite ZSM-5 crystals were obtained. These materials were characterized by powder X-ray diffraction, nitrogen adsorption, electron microscopy, and multi-nuclear solid state NMR spectroscopy. The Brønsted acid-

ity was characterized by ^{1}H and ^{13}C MAS NMR spectroscopy of dehydrated samples.

2. Experimental section

2.1 Preparation of the materials

A hydrogel suitable to synthesize ZSM-5 seeds was prepared by 53.6 g of a 1 M aqueous solution of tetrapropylammonium hydroxide (TPAOH), 0.984 g $NaAlO_2$, 182.88 g H_2O and 16.0 g SiO_2 (fumed silica). This solution was transferred into an autoclave and kept at 323 K for 18 h. The obtained gel was added to 25.2 g cetyltrimethylammonium bromide (CTAB) and stirred (400 min^{-1}) at room temperature for 2 h. Subsequently, the material was heated at 353 K under a stirring rate of 100 min^{-1} for 20 h. The dry gel obtained in this way was ground into a fine powder. An amount of 3.0 g dry gel was placed into the upper part of the autoclave described in [19] with a volume of 130 ml, while 4.0 g of deionized water were put at the bottom of this autoclave. After heating of the dry gel at 423 K for 24 to 72 h, the obtained materials were washed with deionized water and dried at 353 K for 12 h. The obtained samples were denoted MZH-24h to MZH-72h (MZH: MCM-41/ZSM-5 Hybrid).

To remove the template molecules, the samples were heated from room temperature to 393 K with a rate of 1 K/min and kept at 393 K for 3 h. Subsequently, the temperature was raised to 823 K with a rate of 1 K/min, and the material was calcined under a flow of nitrogen (58 l/h) with 20 vol.-% oxygen. The H-form of the samples was obtained by a threefold ion exchange in a 0.1 M aqueous solution of ammonium nitrate and a calcination at 823 K for 8 h.

As a reference material, zeolite ZSM-5 with an n_{Si}/n_{Al} ratio of 22 was synthesized according to [20]. The preparation of the H-form of this sample was performed as described above.

2.2 Characterization methods

X-ray diffraction measurements were performed on a Siemens D5000 instrument in steps of 0.02° using Cu K_α radiation. Nitrogen adsorption/desorption isotherms were recorded with a Micrometrics ASAP 2000 instrument after the samples were dehydrated at 623 K in vacuum for 12 h. The transmission electron microscopic (TEM) images were taken on a Philips STEM 400 electron microscope. A scanning electron micrograph (SEM) was taken on a CAMSCAN 44 electron microscope. Elemental analysis was carried out by AES/ICP using a Perkin Elmer Plasma 400 spectrometer.

NMR investigations were performed on an NMR spectrometer Bruker MSL 400 at resonance frequencies of 400.1 MHz for ^{1}H, 104.2 MHz for ^{27}Al, 100.6 MHz for ^{13}C, and 79.5 MHz for ^{29}Si nuclei. ^{1}H, ^{13}C, and ^{27}Al MAS NMR spectra were recorded with a sample spinning rate of 10 kHz, while a sample

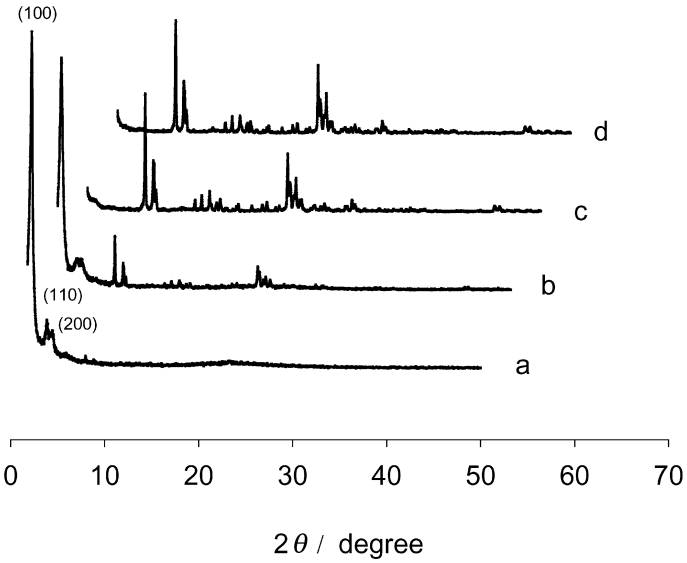

Fig. 1. XRD patterns of the calcined materials obtained after dry-gel conversion at 423 K for 24 h (a), 36 h (b), 48 h (c), and 72 h (d).

spinning rate of 4 kHz was used for ^{29}Si MAS NMR spectroscopy. The repetition times were 0.5 s for ^{27}Al, 5 s for ^{13}C, 10 s for ^{1}H, and 30 s for ^{29}Si MAS NMR spectroscopy. The free induction decays were recorded after single-pulse $\pi/2$ (^{1}H, ^{13}C, ^{29}Si) or $\pi/6$ (^{27}Al) excitation. ^{1}H, ^{13}C, and ^{29}Si MAS NMR spectra were referenced to TMS (tetramethylsilane), while a 1.0 M aqueous solution of aluminum nitrate was used as chemical shift standard for ^{27}Al MAS NMR spectroscopy.

Before the adsorption of probe molecules, the samples were dehydrated at 673 K for 12 h in vacuum ($p < 10^{-2}$ mbar). ^{13}C-2-Acetone was adsorbed by using a standard volume connected to the vacuum line and by cooling the samples in liquid nitrogen. In the case of ammonia adsorption, the samples were saturated with this probe molecule at room temperature. Subsequently, a desorption of the physically adsorbed ammonia was carried out in vacuum ($p < 10^{-2}$ mbar) at 473 K for 2 h.

3. Results and discussion

3.1 X-ray diffraction

Fig. 1 shows the XRD patterns of a series of materials obtained after dry-gel conversion times t of 24 to 72 h. After $t = 24$ and 36 h, the XRD patterns are

dominated by (100), (110), and (200) reflections, indicating the formation of well-defined hexagonal MCM-41 materials. Starting after a dry-gel conversion time of 36 h, the high-angle range XRD pattern contains reflections, which are typical for those of zeolite ZSM-5 crystals [21]. These reflections dominate the pattern for $t \geqslant 48$ h. Hence, a collapse of the hexagonal MCM-41 framework must have occurred at elevated conversion times, during which the material was fully transformed into ZSM-5 crystals.

The XRD patterns of the as-synthesized (not shown) and the calcined materials (Fig. 1) do not show significant differences. This finding suggests the absence of lamellar phases in the as-synthesized material, since such a phase would have been decomposed by a calcination at 823 K. A lamellar phase was observed by Chen *et al.* [22] and Huang *et al.* [16] for mesoporous silica materials synthesized with the template CTAB and for MCM-41/ZSM-5 composites, respectively.

According to the XRD patterns in Fig. 1, only the material obtained after a dry-gel conversion time of 36 h shows characteristic reflections of both the hexagonal MCM-41 material and zeolite ZSM-5 crystals. During the transformation of the amorphous dry gel into a partially crystalline material, the hexagonal MCM-41 framework remained partially intact. By the XRD investigation, however, it cannot be decided whether the sample MZH-36h is a simple mixture of MCM-41 domains and zeolite ZSM-5 crystals or an MCM-41 material with a partially crystalline framework.

3.2 Nitrogen adsorption/desorption isotherms

Fig. 2 shows the nitrogen adsorption/desorption isotherms of the samples MZH-24h and MZH-36h and of zeolite H-ZSM-5 as reference material. The isotherms of MZH-24h and -36h are of type IV showing a steep rise at low relative pressures. Capillary condensation occurs at a relative pressure of *ca.* $p/p_0 = 0.3$ suggesting the presence of mesopores. In agreement with the XRD pattern of the samples MZH-48h and MZH-72h, which consists mainly of reflections of zeolite ZSM-5, no capillary condensation was observed for these samples and the isotherms (not shown) agree with that of zeolite H-ZSM-5.

In Fig. 3, the BJH pore size distributions of the samples MZH-24h and MZH-36h are presented. While the diameters at the maximum of the pore size distribution curve of 2.6 nm for MZH-24h and 2.7 nm for MZH-36h are very similar, a broadening of this curve occurs for the sample obtained after the longer dry-gel conversion time.

The BET surface areas of the samples MZH-24h and MZH-36h are both larger than $1000\,m^2\,g^{-1}$ (Table 1, column 3) and show only a slight decrease with increased dry-gel conversion time. For comparison, the nitrogen adsorption/desorption isotherm of zeolite H-ZSM-5 does not show capillary condensation at all (Fig. 2), and the BET surface area amounts to $300\,m^2\,g^{-1}$ only. The formation of ZSM-5 crystals with increased dry-gel conversion times

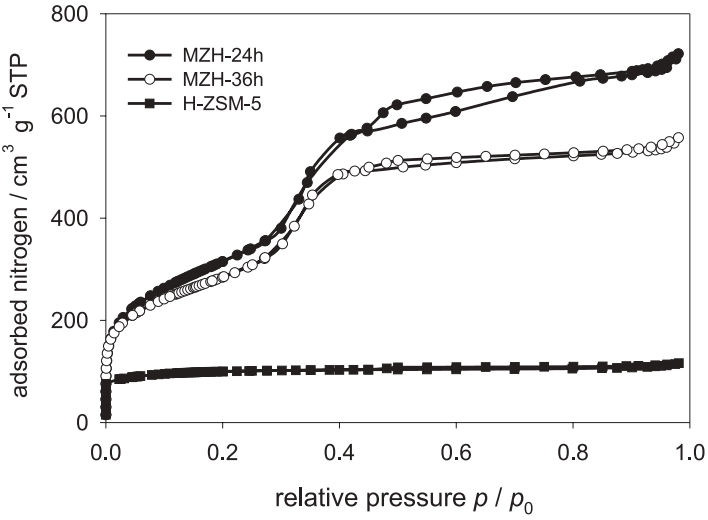

Fig. 2. Nitrogen adsorption/desorption isotherms of the samples MZH-24h and MZH-36h and of zeolite H-ZSM-5.

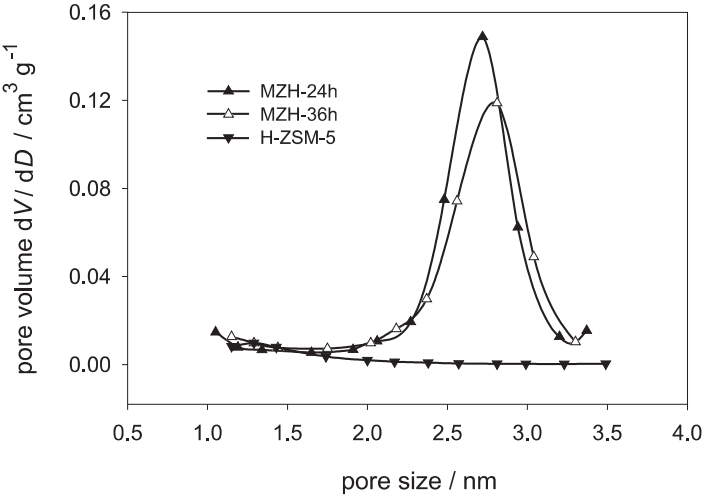

Fig. 3. BJH pore size distributions of the samples MZH-24h and MZH-36h and of zeolite H-ZSM-5.

is accompanied by a slight decrease of the mesopore volume and a significant increase of the micropore volume for sample MZH-36h (Table 1, columns 4 and 5, respectively).

Table 1. Properties of the materials obtained after dry-gel conversion times of 24 and 36 h: n_{Si}/n_{Al} ratios as obtained by AES/ICP (column 2), specific BET surface areas, and mesopore and micropore volumes (columns 4, 5, and 6, respectively) determined by nitrogen adsorption. For comparison, the data of a sample of zeolite H-ZSM-5 are given.

Sample	n_{Si}/n_{Al}	BET surface area /$m^2\,g^{-1}$	$V_{mesopore}$ /$cm^3\,g^{-1}$	$V_{micropore}$ /$cm^3\,g^{-1}$
MZH-24h	59	1248	0.82	0.01
MZH-36h	67	1126	0.76	0.06
H-ZSM-5	22	300	0.06	0.15

3.3 Transmission and scanning electron microscopy

Fig. 4 shows the TEM images of samples MZH-24h and MZH-36h, and the SEM image of sample MHZ-72h. In the TEM image of sample MZH-24h large regions of hexagonally arranged mesopores can be seen. In contrast, after a dry-gel conversion time of 36 h, the arrangement of the mesopores is severely disturbed. Large regions with disordered mesopores and only small regions with hexagonally arranged mesopores occur in Fig. 4b. This finding agrees with the broadening of the low-angle reflections in the XRD pattern of sample MZH-36h in comparison with those of sample MZH-24h.

On the other hand, no particles with typical shapes of zeolite ZSM-5 crystals could be observed for sample MZH-36h. This is consistent with the formation of an MCM-41 material with a partially crystalline framework rather than the formation of a mixture of MCM-41 domains and ZSM-5 crystals. It is only the SEM picture of sample MZH-72h that shows particles with regular shapes similar to those of ZSM-5 crystals (Fig. 4c).

3.4 ^{29}Si and ^{27}Al MAS NMR spectroscopy

By ^{29}Si MAS NMR spectroscopy, the local structure of silicon atoms in the materials was directly investigated. For crystalline aluminosilicates, such as zeolite ZSM-5, well-resolved ^{29}Si MAS NMR spectra consisting of the signals of silicon atoms with different numbers of aluminum atoms in the first coordination sphere of T-atoms (T = Si or Al) were obtained [23–25]. On the other hand, due to the broad distribution of T–O–T angles and T–O bond lengths in the amorphous framework of MCM-41, the ^{29}Si MAS NMR spectra of these materials consist of broad signals at −90 to −110 ppm due to Q^2 and Q^3 silicon atoms coordinated to two and one OH groups, respectively, and Q^4 silicon atoms coordinated to one or no aluminum atoms in the first coordination sphere of T atoms [26–28].

The ^{29}Si MAS NMR spectrum of the as-synthesized dry gel in Fig. 5a consists of two broad signals at −99 and −109 ppm mainly caused by

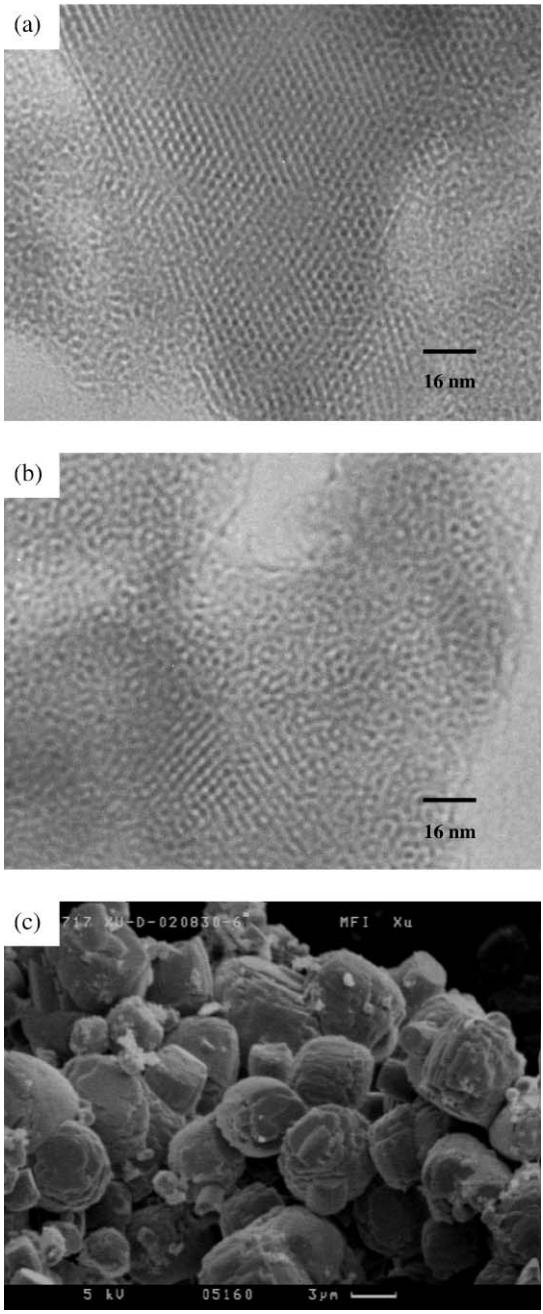

Fig. 4. TEM images of the samples MZH-24h (a) and -36h (b) and SEM picture of the sample MZH-72h (c).

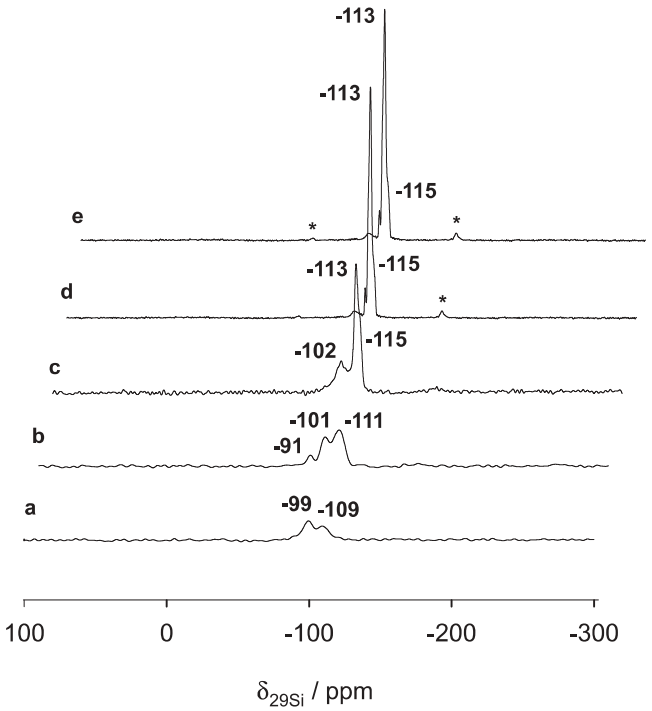

Fig. 5. ^{29}Si MAS NMR spectra of the as-prepared dry gel (a) and of the samples MZH-24h (b), MZH-36h (c), MZH-48h (d), and MZH-72h (e). Asterisks denote spinning sidebands.

Si(3Si,1(OH)) and Si(4Si,0Al) species, respectively (Fig. 5a). It should be noted, that the intensity of the former signal is higher than that of the latter, which indicates that the Si(3Si,1(OH)) species are the dominating silicon species in the dry gel. The ^{29}Si MAS NMR spectrum recorded after a dry-gel conversion time of 24 h is similar to that of a conventionally synthesized MCM-41 material [26–28] with signals at −91, −101, and −110 ppm due to Si(2Si,2(OH)) species, a superposition of Si(3Si,1(OH)) species and Si(3Si,1Al) species, and Si(4Si,0Al) species, respectively (Fig. 5b). The occurrence of the signal of Si(2Si,2(OH)) species in the spectrum of the sample MZH-24h indicates that the initiation of the dry-gel conversion is accompanied by a further break of Si–O–T bonds as a prerequisite for the transformation of the amorphous material. A similar observation was made during the study of the synthesis of zeolite [Ga]Beta via the dry-gel conversion method [19]. In the first step of the dry-gel conversion process, an increase of the concentration of defect SiOH groups was found [19].

In contrast to the ^{29}Si MAS NMR spectrum of the sample MCM-24h in Fig. 5b, the spectrum of the sample MZH-36h consists of a narrow signal at

−113 ppm with a high-field shoulder at *ca.* −115 ppm (Fig. 5c). This narrow ^{29}Si MAS NMR signal is characteristic for Si(4Si,0Al) species in the framework of aluminum-containing zeolite ZSM-5 [23, 29]. The broad low-field signals are much weaker and consist of a signal at −102 ppm due to Si(3Si,1(OH)) and Si(3Si,1Al) species. While the latter species mainly contribute to the parent MCM-41 framework, the former species are localized in crystalline structures. In agreement with the results of XRD diffraction, the ^{29}Si MAS NMR spectra of the samples MZH-48h and MZH-72h are dominated by the narrow signal at −113 ppm (Fig. 5d and e). Only a weak signal of Si(3Si,1Al) species occurs at −102 ppm. The small intensity of this low-field signal indicates a total transformation of the amorphous MCM-41 framework into crystalline local structures without defect SiOH groups occurring as the ^{29}Si MAS NMR signal of Si(3Si,1(OH)) species.

Brønsted acid sites in zeolites are closely related to the presence of tetrahedrally coordinated aluminum species incorporated at T positions into the framework leading to the formation of bridging hydroxyl groups (SiOHAl) [30, 31]. Tetrahedrally coordinated framework aluminum atoms of hydrated zeolites cause ^{27}Al MAS NMR signals in the range of 55 to 60 ppm [23, 32]. In the present study, already the ^{27}Al MAS NMR spectrum of the as-prepared dry-gel was dominated by a signal at 50 ppm corresponding to tetrahedrally coordinated aluminum species (not shown). After a dry-gel conversion time of 24 h, this signal shifted to 54 ppm and no further change of the ^{27}Al MAS NMR spectra was found after the dry-gel conversion time was increased to 36, 48, and 72 h.

3.5 NMR investigations of Brønsted acid sites

^{1}H MAS NMR spectroscopy allows a direct study of Brønsted acid sites in dehydrated solid catalysts [30, 31]. Defect SiOH groups, which are typical for amorphous materials, occur at resonance positions of 1.3 to 2.2 ppm. Acidic bridging OH groups, such as observed in the ^{1}H MAS NMR spectra of dehydrated zeolite H-ZSM-5, have a chemical shift of *ca.* 4.0 ppm [30, 31].

In Fig. 6, the ^{1}H MAS NMR spectra of the dehydrated samples MZH-24h to MZH-72h are depicted. The spectrum of the material obtained after a dry-gel conversion time of 24 h consists exclusively of a strong signal at 1.8 ppm, indicating the presence of a large number of defect SiOH groups (Fig. 6a). Starting at a dry-gel conversion time of 36 h, a weak low-field shoulder emerges at *ca.* 4 ppm, which indicates the formation of bridging OH groups (Fig. 6b). After dry-gel conversion times of 48 and 72 h, this signal has increased significantly, while the signal of defect SiOH groups has strongly decreased (Fig. 6c and d). The ^{1}H MAS NMR spectra of the samples MZH-48h and MZH-72h agree well with those of conventionally synthesized zeolites H-ZSM-5 [30, 31, 33].

For a determination of the concentration of Brønsted acid sites of the sample MZH-36h, ammonia was loaded onto the dehydrated material. Subse-

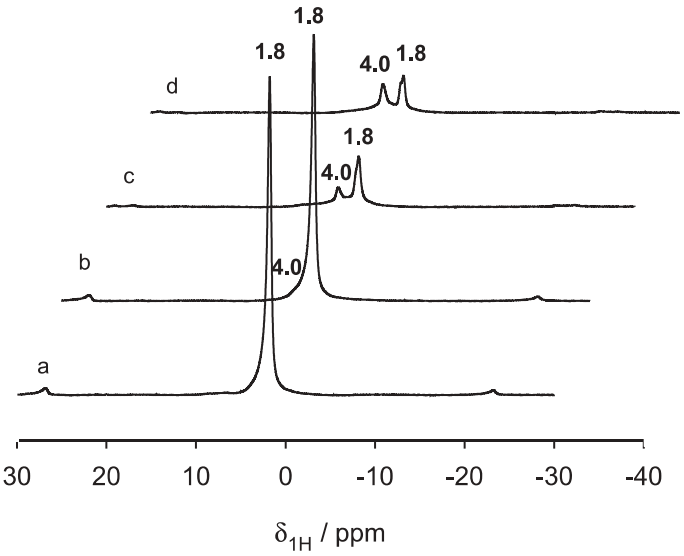

Fig. 6. ^{1}H MAS NMR spectra of the dehydrated samples MZH-24h (a), MZH-36h (b), MZH-48h (c), and MZH-72h (d).

quently, the intensity of the ^{1}H MAS NMR signal of ammonium ions occurring at *ca.* 6.5 ppm was quantitatively evaluated. In this way, a concentration of Brønsted acid sites of 0.1 mmol per gram of dehydrated powder was determined.

The strength of Brønsted acid sites in sample MZH-36h was characterized using acetone as a probe molecule. As demonstrated by Biaglow *et al.* [34, 35] and Barich *et al.* [36], the ^{13}C NMR shift of the carbonyl groups in ^{13}C-2-acetone molecules bound to Brønsted acid sites enables a ranking of the acid strength of solid materials. The ^{13}C MAS NMR spectrum of ^{13}C-2-acetone adsorbed on the dehydrated sample MZH-36h consists of two signals at 223 and 233 ppm (Fig. 7a). The signal at 233 ppm is ascribed to the carbonyl groups of acetone molecules coordinated to Lewis acid sites, such as observed by Biaglow *et al.* [35] for acetone adsorbed on dealuminated zeolite H-Y. The resonance position of the ^{13}C MAS NMR signal at 223 ppm agrees with that of carbonyl groups of acetone molecules bound to Brønsted acid sites in zeolite H-ZSM-5. As a comparison, Fig. 7b shows the ^{13}C MAS NMR spectrum of zeolite H-ZSM-5 loaded with ^{13}C-2-acetone. The agreement of the ^{13}C NMR shifts of acetone molecules adsorbed on zeolite H-ZSM-5 with those adsorbed on the sample MZH-36h gives evidence for the high strength of Brønsted acid sites in the material obtained by the dry-gel conversion method.

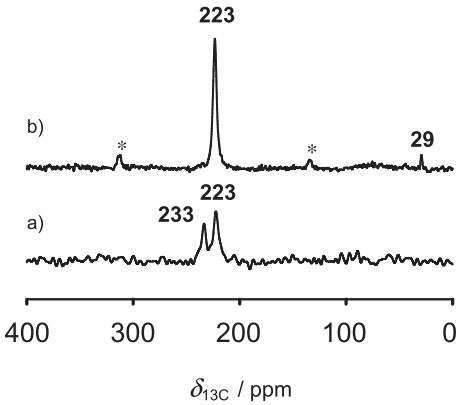

Fig. 7. ^{13}C MAS NMR spectra of the dehydrated sample MZH-36h (a) and a dehydrated zeolite H-ZSM-5 (b) recorded after adsorption of ^{13}C-2-acetone as probe molecule. Asterisks denote spinning sidebands.

4. Conclusions

For the first time, the dry-gel conversion method was applied to prepare MCM-41 materials with partially crystalline framework. For this purpose, a hydrogel suitable for the synthesis of zeolite ZSM-5 seeds was added to a solution of cetyltrimethylammonium bromide and heated to obtain a dry gel. This dry gel was converted for different times and, subsequently, characterized by powder X-ray diffraction, nitrogen adsorption, electron microscopy, and multi-nuclear solid state NMR spectroscopy.

Starting after a dry-gel conversion time of 36 h, the XRD pattern of the obtained material consisted of reflections of the mesoporous MCM-41 material and zeolite ZSM-5 crystals. By nitrogen adsorption, a BET surface area of 1126 m^2/g and mesopore and micropore volumes of 0.76 and 0.06 cm^3/g, respectively, were determined. These data indicate that the mesoporous structure remains during the dry-gel conversion, while a significant micropore volume is formed. The ^{29}Si MAS NMR spectrum of the material obtained after a dry-gel conversion time of 36 h consists of a broad signal of Q^3 silicon species at framework defects and a narrow signal of Q^4 silicon species in crystalline local structures such as in zeolite ZSM-5. The TEM image of this sample shows mesopores in a disturbed arrangement, but no ZSM-5 crystals. These findings might be an indication that the framework of the mesoporous MCM-41 material obtained after the dry-gel conversion time of 36 h is partially transformed into a crystalline one without forming a separate zeolitic phase. Upon increasing the dry-gel conversion time to 48 and 72 h, an extensive to total transformation of the amorphous dry gel into zeolite ZSM-5 crystals was found.

^{1}H MAS NMR spectroscopy of the material obtained after a dry-gel conversion time of 36 h indicates the formation of hydroxyl groups with a chemical shift of *ca.* 4 ppm and a concentration of *ca.* 0.1 mmol/g. The acid strength of these hydroxyl groups, as studied by ^{13}C MAS NMR spectroscopy of adsorbed acetone, was found to agree with that of bridging OH groups in zeolite H-ZSM-5. Further investigations will be devoted to the catalytic properties of the MCM-41/ZSM-5 materials obtained via the dry-gel conversion method.

Acknowledgement

Financial support by Deutsche Forschungsgemeinschaft, Max-Buchner-Forschungsstiftung, and Fonds der Chemischen Industrie is gratefully acknowledged. We thank Michael Froeba, Institute of Inorganic and Analytical Chemistry, Justus Liebig University Giessen, for recording the TEM images.

References

1. T. Yanagisawa, T. Shimizu, K. Kuroda, and C. Kato, Bull. Chem. Soc. Jpn. **63** (1990) 988.
2. C. T. Kresge, M. E. Leonowicz, W. J. Roth, J. C. Vartuli, and J. S. Beck, Nature **359** (1992) 710.
3. S. Biz and M. L. Occelli, Catal. Rev.-Sci. Eng. **40** (1998) 329.
4. P. Selvam, S. K. Bhatia, and C. G. Sonwane, Ind. Eng. Chem. Res. **40** (2001) 3237.
5. G. Øye, J. Sjoeblom, and M. Stoecker, Adv. Coll. Interf. Sci. **89** (2001) 439.
6. A. Ghanbari-Siahkali, A. Philippou, A. Garforth, C. S. Cundy, M. W. Anderson, and J. Dwyer, J. Mater. Chem. **11** (2001) 569.
7. M. Xu, W. Wang, M. Seiler, A. Buchholz, and M. Hunger, J. Phys. Chem. B **106** (2002) 3202.
8. X. S. Zhao, G. Q. Lu, and C. Song, Chem. Commun. (2001) 2306.
9. V. R. Choudhary and K. Mantri, J. Catal. **205** (2002) 221.
10. M. Xu, A. Arnold, A. Buchholz, W. Wang, and M. Hunger, J. Phys. Chem. B **106** (2002) 12 140.
11. Z. Zhang, Y. Han, L. Zhu, R. Wang, Y. Yu, S. Qiu, D. Zhao, and F. Xiao, Angew. Chem. **113** (2001) 1298.
12. Y. Liu, W. Zhang, and T. J. Pinnavaia, J. Am. Chem. Soc. **122** (2000) 8791.
13. Y. Liu, W. Zhang, and T. J. Pinnavaia, Angew. Chem. **113** (2001) 1295.
14. A. Karlsson, M. Stoecker, and R. Schmidt, Microporous Mesoporous Mater. **27** (1999) 181.
15. R. W. Thompson, in *Molecular Sieves, Science and Technology, Vol. 1*, H. G. Karge and J. Weitkamp (Eds.), Springer-Verlag, Berlin (1998), p. 1.
16. L. Huang, W. Guo, P. Deng, Z. Xue, and Q. Li, J. Phys. Chem. B **104** (2000) 2817.
17. W. Xu, J. Dong, J. Li, and F. Wu, J. Chem. Soc., Chem. Commun. (1990) 755.
18. M. Matsukata, M. Ogura, T. Osaki, P. R. H. P. Rao, M. Nomura, and E. Kikuchi, Top. Catal. **9** (1999) 77.
19. A. Arnold, S. Steuernagel, M. Hunger, and J. Weitkamp, Microporous Mesoporous Mater. **62** (2003) 97.
20. S. Ernst and J. Weitkamp, Chem. Ing. Tech. **63** (1991) 748.

21. M. M. J. Treacy and J. B. Higgins, *Collection of Simulated XRD Powder Patterns for Zeolites*, 4th Edition, Elsevier, Amsterdam (2001), p. 234.
22. X. Chen, L. Huang, and Q. Li, J. Phys. Chem. B **101** (1997) 8460.
23. G. Engelhardt and D. Michel, *High-resolution Solid-State NMR of Silicates and Zeolites*, J. Wiley & Sons: New York, Toronto (1987), p. 158.
24. C. A. Fyfe, G. C. Gobbi, J. Klinowski, J. M. Thomas, and S. Ramdas, Nature **296** (1982) 530.
25. C. A. Fyfe, H. Strobl, G. T. Kokotailo, G. J. Kennedy, and G. E. Barlow, J. Am. Chem. Soc. **110** (1988) 3373.
26. W. Guo, C. Xiong, L. Huang, and Q. Li, Mater. Chem. **11** (2001) 1886.
27. X. S. Zhao, M. G. Q. Lu, and C. Song, J. Mol. Catal. A: Chem. **191** (2003) 67.
28. M. Hunger, U. Schenk, M. Breuninger, R. Glaeser, and J. Weitkamp, Microporous Mesoporous Mater. **27** (1999) 261.
29. C. A. Fyfe, G. C. Gobbi, and G. J. Kennedy, J. Phys. Chem. **88** (1984) 3248.
30. M. Hunger, Solid State Nucl. Magn. Reson. **6** (1996) 1.
31. M. Hunger, Catal.-Rev. Sci. Eng. **39** (1997) 345.
32. H. G. Karge, M. Hunger, and H. K. Beyer, in *Catalysis and Zeolites, Fundamentals and Applications*, J. Weitkamp and L. Puppe (Eds.), Springer-Verlag, Berlin (1999), p. 198.
33. M. Hunger, D. Freude, T. Froehlich, H. Pfeifer, and W. Schwieger, Zeolites **7** (1987) 108.
34. A. I. Biaglow, R. J. Gorte, G. T. Kokotailo, and D. White, J. Catal. **148** (1994) 779.
35. A. I. Biaglow, R. J. Gorte, and D. White, J. Catal. **150** (1994) 221.
36. D. H. Barich, J. B. Nicholas, T. Xu, and J. F. Haw, J. Am. Chem. Soc. **120** (1998) 12 342.